

ZnO nanorods grown on p-GaN using hydrothermal synthesis and its optoelectronic devices application

LE Hong Quang², CHUA Soo Jin^{1,2}, Eugene FITZGERALD³, LOH Kian Ping⁴

¹Centre for Optoelectronics, National University of Singapore, Engineering Drive 3, Singapore

²Singapore-MIT-Alliance, National University of Singapore, Singapore

³Department of Electrical and Computer Science, Massachusetts Institute of Technology, Cambridge, Massachusetts, USA

⁴Chemistry Department, National University of Singapore

Abstract —The ZnO nanorods with the length of 1-1.5 μm were deposited on p-GaN by hydrothermal synthesis at low temperature 100°C. The structural and optical properties of the as-grown ZnO rods were investigated by X-Ray diffraction (XRD) and photoluminescence (PL) spectra. After annealing treatment the as-grown films in air at 600°C, 30min, and the ZnO rods showed good crystallinity and optical properties with strong UV emission at 378 nm. In addition, a sharp UV emission peak at 369.45 nm with the FWHM 20 meV, which attributed to the bound exciton recombination, was also observed from the ZnO rods at 80K. Next, the e-beam evaporation method was used to deposit metal contact on n-ZnO and p-GaN. Here, we use Au and Ni/Au as metal contacts for n-ZnO and p-GaN, respectively. The current-voltage characteristics of the fabricated n-ZnO/p-GaN heterojunction revealed rectifying behavior with a leakage current of 10^{-8} A at -10V, a forward current 4×10^{-6} A at 10V bias. The heterojunction also showed a good photoresponse, with the change of the current – voltage characteristics under ultraviolet illumination. Under UV illumination, the forward turn on voltage changed to 7.5V. This result showed the ability to manipulate the electron transport in the ZnO based heterojunction devices.

Index Terms —II-VI material, nanostructure, heterostructure, hydrothermal

ZnO is a promising material for short-wavelength photonic device application due to its novel characteristics such as direct and wide band gap, large exciton binding energy of 60 meV. From the literature, both ZnO epitaxial films and single crystal nanorods have shown excellent optical properties [1,2]. Further more, some research on ZnMgO alloys showed the ability to control the band gap energy of ZnO-based materials and the fabrication of ZnO/ZnMgO nanorod quantum structures [3]. Despite the significant progress on ZnO films and nanostructures, the fabrication of ZnO p-n homojunction devices has been inhibited by the difficulty of fabrication stable and high quality p type doping ZnO.

As an alternative approach to homojunction, an n-ZnO/p-GaN heterojunction has been considered as a strong candidate for device applications [4]. since these materials have a similar bandgap energy (3.38 eV for ZnO, 3.4 eV for GaN), the same wurtzite crystal structure and a low lattice constant misfit of 1.9%. In general, however, p-n heterojunction devices show a lower efficiency than homojunction devices [5,6], because an energy barrier formed at the junction interface decreases carrier injection efficiency for heterojunction with large band offset [7]. However, by making nanosized junctions, the carrier injection efficiency could be increased since, as previously reported, the carrier injection rate significantly increase for nanocontacts in Schottky diodes [8,9]. In this paper, we will report on the fabrication of n-ZnO nanorods/p-GaN heterostructure and its characteristics.

A schematic of n-ZnO/pGaN heterostructure is shown in Figure 1. Firstly, 1 μm thick p-GaN was grown on sapphire substrate by our MOCVD system at 1020°C. This p-GaN would be used as a template to grow n-ZnO nanorods on the top and also used as a p layer in the n-ZnO/p-GaN heterostructure. Then, vertically well aligned n type ZnO nanorod arrays were epitaxially grown on p type GaN (0001) substrates employing catalyst free hydrothermal synthesis method. The growth and characteristic of ZnO nanorods grown on GaN has been reported elsewhere [7,8,9]. The synthesis of ZnO nanorods results in a preferential growth direction along the c-axis of ZnO normal to the substrate surface. Field emission scanning electron microscopy (FESEM) revealed the general morphology of the ZnO nanorod arrays on p-GaN. The ZnO nanorod arrays have uniform distribution in diameter and length. The average length and diameter of the nanorods grown for 4h are 2 μm and 80nm, respectively. The number density of nanorods was as high as 10^9 per cm^2 .

After the growth of ZnO nanorods on GaN, an insulating layer (polystyrene) was filled in the gaps between the nanorods by spin coating method. This insulating layer will help to prevent the carrier transport

from one rod to the others and ensure the injection carrier transport along the rod to the p type GaN. The thickness of the insulating layer had to be shorter than the length of the ZnO nanorod so that the tip of the ZnO rods was still exposed (SEM image in the diagram). After that, part of the sample was etched to expose the p-GaN. In was deposited on n-ZnO and Ni/Au were evaporated on p-GaN. Good Ohmic contacts on both n-ZnO and p-GaN were made by rapid thermal annealing. Finally, four probe systems were used to characterize the current-voltage behavior of n-ZnO/p-GaN heterostructure.

It has been known that metallic composition of the contact is a critically important parameter for making Ohmic contacts to n-ZnO and p-GaN. Here, In was chosen as a metal contact on ZnO due to its smaller work function (for In $\Phi_m = 4.12\text{eV}$;for ZnO $\Phi_m = 5.2$) Figure 2 showed the I-V characteristic of In contact on ZnO. It show ohmic behavior which revealed In as a ohmic contact for ZnO. Ni/Au was used as metal contacts on p-GaN. An annealing process at high temperature in a nitrogen or oxygen environment was necessary to decrease contact resistance and to increase adhesive force. The I-V characteristics of Ni/Au contact on p-GaN before and after thermal annealing treatment (300°C in air) were shown in Figure 2. After annealing, the resistivity of Ni/Au contact decreased from $5.5\text{ K}\Omega$ to $2.2\text{ K}\Omega$. This value is still high and more experiments are needed to achieve lower resistivity. For the In contact, the difference in I-V characteristic of the contact before and after annealing is not so significant.

The n-ZnO/p-GaN heterostructure's band diagram was constructed by following the Anderson model. The schematic of n-ZnO/pGaN heterojunction's band diagram was shown in Figure 3 (a).

The energy barrier for electron is $\Delta E_c = 0.15\text{eV}$, and for hole

$$\Delta E_v = E_g(\text{ZnO}) + \Delta E_c - E_g(\text{GaN}) = 3.37 + 0.15 - 3.39 = 0.13\text{eV}.$$

The band bending can be calculated as

$$V_D = E_{Fp} - E_{Fn} = (\chi_{\text{GaN}} + E_g(\text{GaN}) - \delta_{\text{GaN}}) - (\chi_{\text{ZnO}} + \delta_{\text{ZnO}})$$

By assuming that $\delta_{\text{ZnO}} = E_c - E_F = 0.1\text{eV}$ and $\delta_{\text{GaN}} = E_F - E_v = 0.1\text{eV}$, we can roughly calculate

$$V_D = (\chi_{\text{GaN}} + E_g(\text{GaN}) - \delta_{\text{GaN}}) - (\chi_{\text{ZnO}} + \delta_{\text{ZnO}}) \\ = (4.2 + 3.39 - 0.1) - (4.35 + 0.1) = 3.24\text{ eV}.$$

Therefore, a rectifying behavior was expected from the I-V characteristic of the n-ZnO/p-GaN heterostructure. This is consistent with the experiment result shown in figure 3 (b). It also shows a threshold voltage of 6.5V and a low leakage current of $2 \times 10^{-8}\text{A}$ with soft break down .The measured threshold voltage from our heterostructure had a higher value than the band bending due to neglecting the effects of dipole and interfacial state. This kind of interfacial state has become more severe under hydrothermal growth condition (low temperature growth). Another feature of the I-V characteristics, which is noteworthy , is that our heterostructure does not conform to the "normal" forward bias relationship in which the current depends exponentially on the voltage divided by a product of the thermal energy times an ideality factor of $n=1$ (high injection regime) or $n=2$ (series resistance regime) [17]

$$I \sim \exp(qV/nkT) \quad (*)$$

The I-V characteristic in figure 3.b was replotted in $\ln I$ vs V in order to fit the normal forward bias relationship (*). A significant portion of the $\ln I$ - V curve can be well fit using $n=15$ (figure 4). An n of such a large magnitude argues against the feasibility of employing an exponential relationship to account for this I-V trend.

The log-log plot of the I-V data for the n-ZnO nanorods/p-GaN sample is shown in figure 5. The current transport show Ohmic behavior ($I \sim V$) for the applied forward voltage smaller than 1.5V . As the applied voltage is larger than 1.5V , the current transport deviates from Ohmic behavior and with applied bias larger than 3.5V , it follow the dependence of $I \sim V^2$. The $I \sim V^2$ transport of the n-ZnO nanorod/p-GaN can not be explained by heterojunction band structure model space charge limited (SCL) current conduction has been observed in various semiconductor structure [18,19,20]. Lambort and Mark have developed the single carrier SCL current model with the presence of a trap above the Fermi level. [21]. This model provide insight into the operative mechanism responsible for the I-V trends of n-ZnO/p-GaN heterostructure.

As the applied voltage is lower than the onset voltage V_{on} ($V_{on} < 1.5\text{v}$) for deviating from Ohmic behavior , the thermally generated carrier density and the carrier transit time $\tau_c = d^2/\mu V_{on}$ is larger than the dielectric relaxation time $\tau_d = \epsilon / qn \mu$. The injected carrier would undergo dielectric relaxation to maintain the charge neutrality rather than transport across the sample. In this region, the traps are not completely filled. As the applied voltage is larger than V_{on} , τ_c is smaller than τ_d and the injected carrier dominates over the thermally generated carrier. The increase of applied voltage will shift the quasi-Fermi level towards the conduction band and the effect would be the filling up of the trap. As the applied voltage further increases to the extent that all the traps are filled ($V > V_{TFL} = 3.5\text{V}$) the conduction would become space charge limited and the current follows the dependence of $I \sim (9/8) \epsilon \mu V^2/d^3$, where d is the thickness of the active region.

An ideal space charge limited current (SCLC) is observed when carriers are injected from contacts into a perfect insulator (wide band gap semiconductor). Since the ideal insulator contains no free carriers in equilibrium, these injected carriers establish space charge in the insulator bulk. Further carrier injection is inhibited by the presence of this injected space charge, giving rise to $I \sim V^2$ square law characteristics. In practice, some free carriers are present in equilibrium so that ohmic conduction dominates the I-V characteristic at the smallest applied voltages. Besides, because of nonidealities such as bulk trap distributions, SCLC behavior is often found to be proportional to a power of the applied voltage greater than 2, as observed in the transition region of the $\log(I)$ - $\log(V)$ curve shown in figure 8.6 in which $I \sim V^{2.5}$.

n-ZnO nanorod/p-GaN heterostructure was fabricated by using hydrothermal synthesis to grow ZnO

on p-GaN sample. The I-V characteristic of this heterostructure show rectifying behavior with low leakage current. The current is proportional to V^2 , which is a typical behavior of the space charge limited current phenomenon. The I-V characteristic of the n-ZnO nanorod/n-GaN heterostructure is found to be ohmic and nearly linear. It clearly confirm that the rectifying diode-like behavior of the n-ZnO/pGaN junction results from the electrical nature of components of the n-p heterojunction , rather than from some interface or contact related phenomena. Here , we only observe the diode characteristic from the n-ZnO/pGaN heterojunction, but not on the emission characteristics. This may be due to the quality of the Ohmic contact on p-GaN , the quality of p-GaN itself and also the interface between ZnO nanorod and p-GaN layer.

References:

- [1] S.W.Jung, W.I.Park, H.D.Cheong, G.C.Yi, Appl.Phys.Lett 2002, 80, 1924
- [2] M.H.Huang, S.Mao, H.Feick, H.Yan, Science 2001 292 1897
- [3] W.I.Park, G.C.Yi, M.Kim, Adv. Mater. 2003 15 526
- [4] S.K.Hong, T.Hanada, H.Makino, Y.Chen, Appl Phys.Lett 2001 78 3349
- [5] X.Duan, Y.Huang, Y.Cui, J.Wang Nature 2001 409 66
- [6] X.Duan , Y.Huang, R.Agarwal, C.M.Lieber Nature 2003 421 241
- [7] M.W.Wang, J.O.Mc Caldin, J.F.Swenberg, T.C.McGill, R.J.Hausnstein, Appl Phys Lett 1995, 66, 1974 .
- [8] J.G.D.J.Smit, S.Rogge, T.M.Klapwijk, Appl. Phys. Lett. 2002 81 3852
- [9] W.I.Park, G.C.Yi, J.W.Kim, S.M.Park Appl Phys Lett 2003 82 4358
- [10] H.Q.Le, S.J.Chua, E.A.Fitzgerald, et al Appl. Phys.Lett. 87 101908 2005
- [11] H.Q.Le, S.J.Chua, E.A.Fitzgerald, et al Nanotechnology 17 483-488 2006
- [12] H.Q.Le, S.J.Chua, E.A.Fitzgerald, et al Journal of crystal growth 287 157-161 2006
- [13] A.G.Milnes, D.L.Feucht, Heterojunctions and Metal Semiconductor Junctions Academic , New York 1972
- [14].A.Aranovich, D.G.Golmayo, A.L.Fahrenbruch, R.H.Bube, J.Appl.Phys 51 4260 1980
- [15] D.Qiao, L.S.Yu, S.S.Lau, J.M.Redwing, J.Y.Lin and H.X.Jiang, J.Appl.Phys. 87 801 2000
- [16] B.M.Ataev, Ya.I.Alivov , Journal of Optoelectronics and Advanced Materials
- [17] S.M.Sze, Physics of Semiconductor devices 2nd ed Wiley New York 1981
- [18] O.J.Marsh and C.R.Viswanathan, J.Appl Phys 38 3135 1967 ,
- [19] H.P.hall, M.A.Awaah and K.Das, Phys Status Solidi A 201 522 2004,m
- [20] R.L.Hoffman, J.F.Wagner, M.K.Jayaraj and J.Tate, J.Appl Phys 90, 5763 2001.
- [21] M.A.Lampert and P.Mark, Current Injection in Solids Academic New York 1970

FIGURES

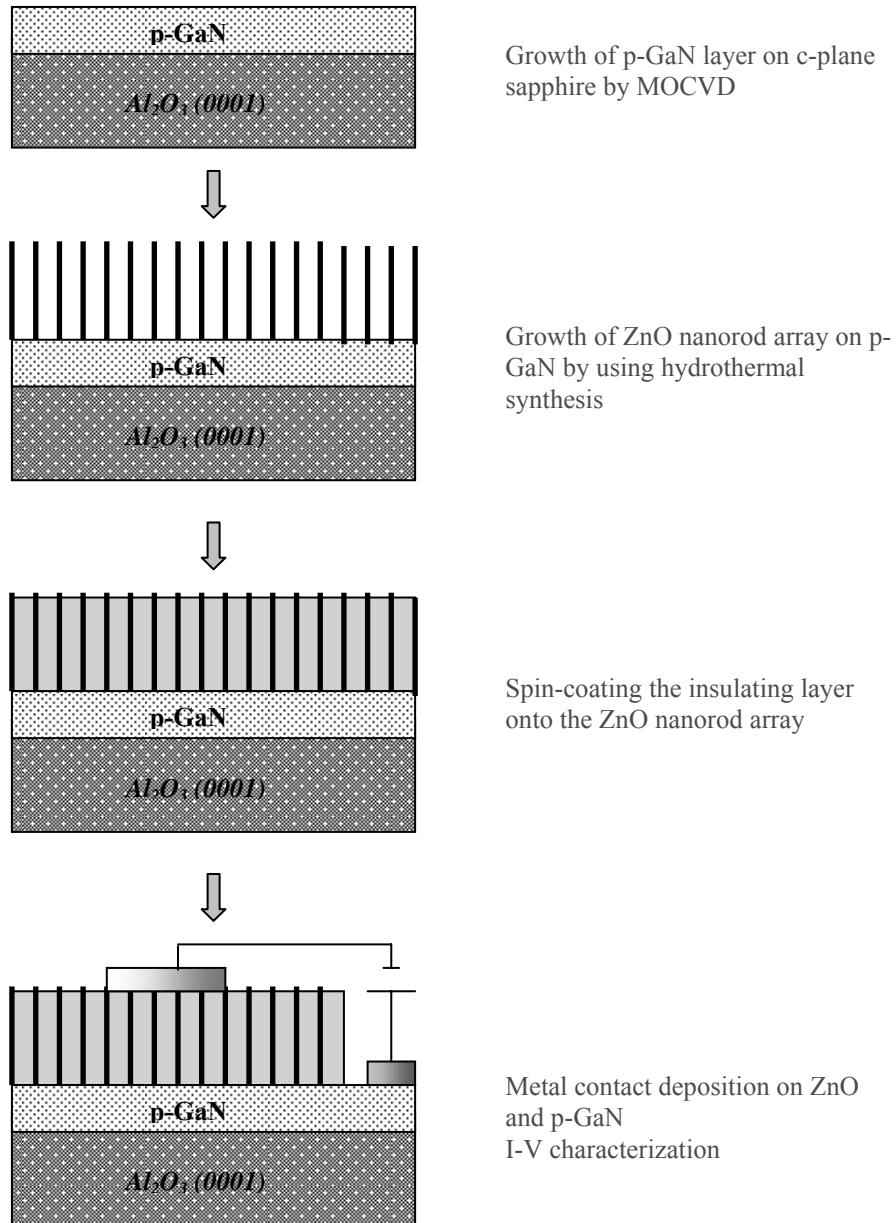


Figure 1: Schematic illustration of a n-ZnO nanorods/p-GaN heterostructure

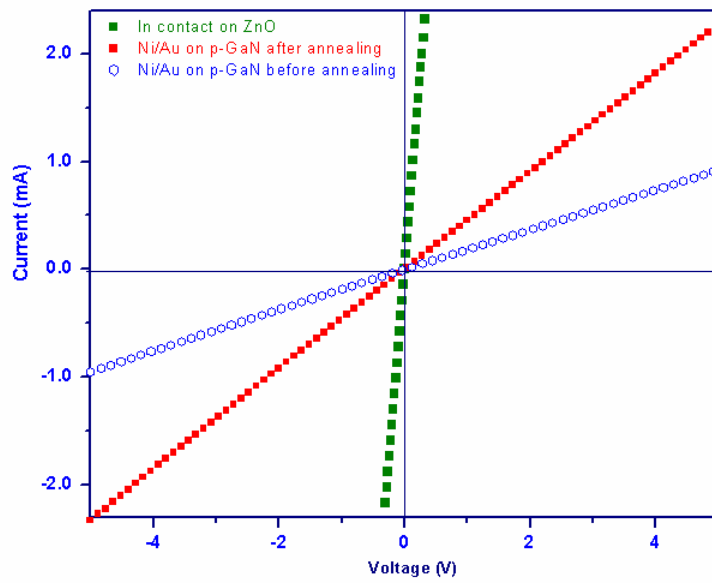


Figure 2. I-V characteristics of In on ZnO, Ni/Au on p-GaN before and after annealing

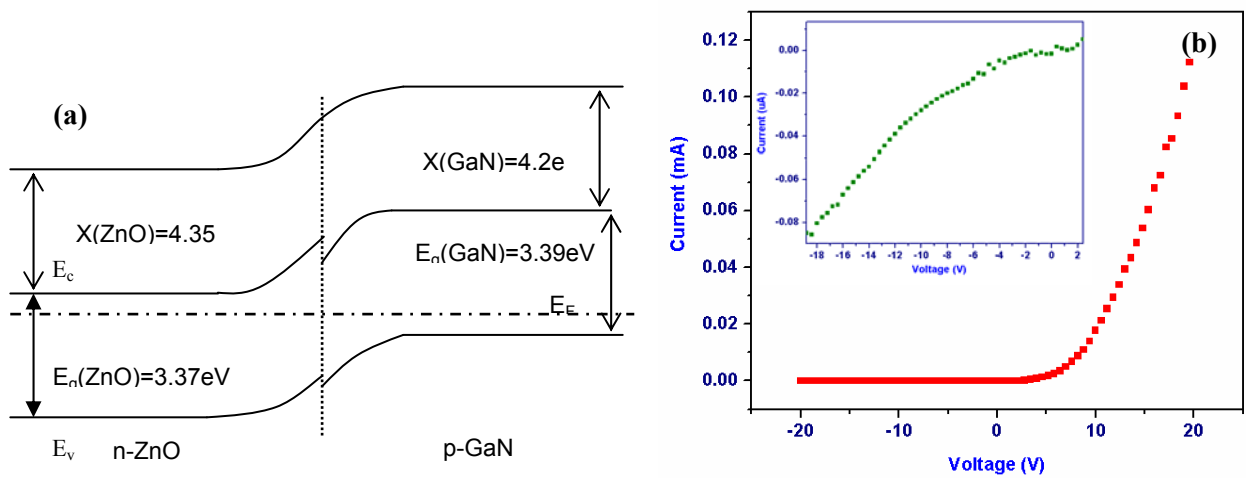


Figure 3 (a) Energy band diagram of the n-ZnO nanorod/p-GaN heterostructure (b) I-V characteristics of the n-ZnO nanorod/p-GaN heterostructure – the inset : I-V characteristic under reverse bias

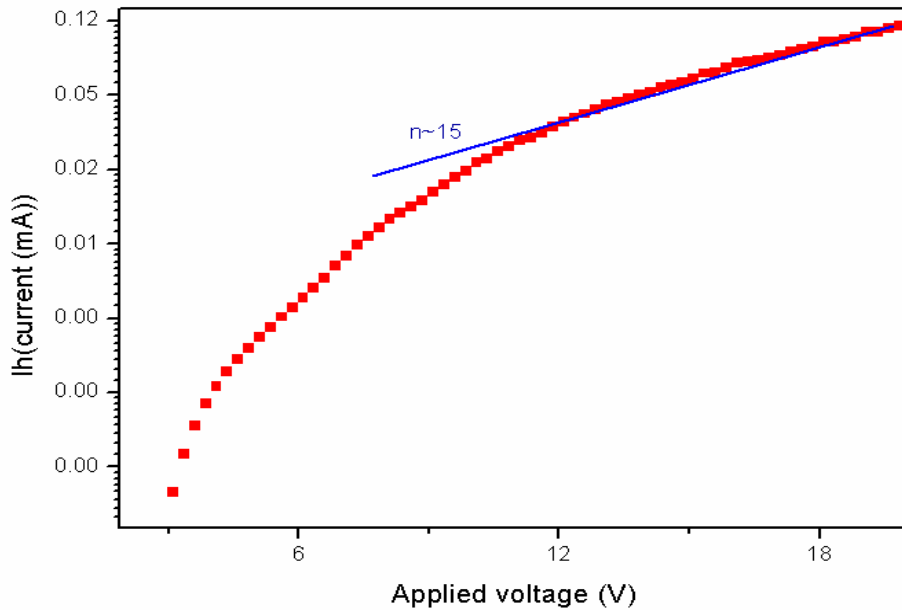


Figure 4: Forward bias $\ln(I)$ - V characteristics of n -ZnO nanorod/ p -GaN heterostructure .

Exponential fit line correspond to ideality factor $n=15$

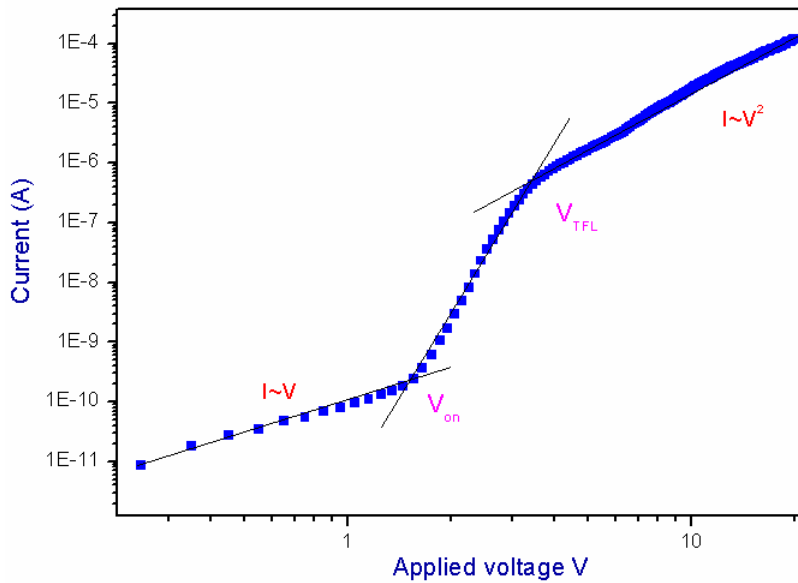


Figure 5. The log-log plot for the I - V data of the n -ZnO nanorod/ p -GaN sample at room temperature